peaks excited by an elastic deformation is much lower for $\lambda = 1{\cdot}54 \times 10^{-1}$ nm compared with $\lambda = 1{\cdot}05 \times 10^{-1}$ nm, the peaks can be experimentally eliminated by choosing a suitable azimuthal angle Φ.

The comparison of the experimental results with the theoretical ones in Table 1, as well as the proof of the quadratic intensity dependence on the vibration amplitude ($I \simeq u_0^2$), show that the developed lamellae model successfully explains the basic phenomena of multiple diffraction observed in an elastically deformed single crystal.

The authors wish to thank Miss B. Hašková and Mr A. Dvořák for their help in preparing the manuscript.

References

AZÁROFF, L. V., KAPLOW, R., KATO, N., WEISS, R. J., WILSON, A. J. C. & YOUNG, R. A. (1974). *X-ray Diffraction*. New York: McGraw-Hill.

BORMANN, G. & HARTWIG, W. (1965). *Z. Kristallogr.* **121**, 401–409.

BURAS, B., GIEBUŁTOWICZ, T., MINOR, W. & RAJCA, A. (1972). *Phys. Status Solidi A*, **9**, 423–433.

CADY, W. (1946). *Piezoelectricity*. New York: McGraw-Hill.

COLE, H., CHAMBERS, F. W. & DUNN, H. M. (1962). *Acta Cryst.* **15**, 138–144.

MICHALEC, R., CHALUPA, B., SEDLÁKOVÁ, L., MIKULA, P., PETRŽÍLKA, V. & ZELENKA, J. (1974). *J. Appl. Cryst.* **7**, 588–592.

MICHALEC, R., MIKULA, P. & VRÁNA, M. (1975). *Proceedings of the Fourth Conference of Czechoslovak Physicists, Liberec*. Prague: Academia.

MIKULA, P., MICHALEC, R. & VÁVRA, J. (1976). *Nucl. Instrum. Methods*, **137**, 23–27.

MIKULA, P., VRÁNA, M., MICHALEC, R. & VÁVRA, J. (1979). *Acta Cryst.* A**35**, 962–965.

MOON, R. M. & SHULL, C. G. (1964). *Acta Cryst.* **17**, 805–812.

PETRŽÍLKA, V., MICHALEC, R., CHALUPA, B., SEDLÁKOVÁ, L., MIKULA, P. & ČECH, J. (1975). *Nucl. Instrum. Methods*, **123**, 353–361.

PETRŽÍLKA, V., VRZAL, J., MICHALEC, R., CHALUPA, B., MIKULA, P. & ZELENKA, J. (1970). *Phys. Status Solidi*, **42**, 895–902.

RENNINGER, M. (1937). *Z. Phys.* **106**, 141–176.

TAKAGI, S. (1969). *J. Phys. Soc. Jpn*, **26**, 1239–1253.

THOMPSON, P. & GRIMES, N. W. (1977). *J. Appl. Cryst.* **10**, 369–371.

Acta Cryst. (1981). A**37**, 465–471

Thin-Crystal Approximations in Structure Imaging

BY P. PIROUZ*

Department of Metallurgy, Faculty of Engineering, University of Tehran, PO Box 1558, *Tehran, Iran*

(*Received* 28 *April* 1980; *accepted* 9 *January* 1981)

Abstract

Starting with the expression for the intensity distribution in a structure image, it is shown that, for a very thin crystal and constant value of the transfer function, there is a one-to-one correspondence between the image and the projection of potential distribution in the crystal along the beam direction. This is formally equivalent to the treatment of weak phase objects by Cowley & Iijima [*Z. Naturforsch. Teil A*, (1972), **27**, 445–451]. With a better approximation, applicable to slightly thicker crystals, it is shown that the image contrast is related not only to the projected potential distribution, but to the square of this function and the projected charge density. Simulated structure images of a silicon crystal, oriented with its [011] direction parallel to the incident beam, show that the distance between the closely spaced spots is increased along the [001] direction, in agreement with experimental images, which is a consequence of not enough diffracted beams contributing to the image as a result of spatial and temporal incoherence of the incident electron beam.

1. Introduction

Cowley & Iijima (1972) showed that, at the proper defocus, there is a direct correlation between the intensity distribution in a structure image of a very thin crystal and the projection of the crystal structure. Their analysis was based on the expansion of the transmission function of a phase object, which represents the change of phase of the electron wave on traversing the

* Presently at: Department of Metallurgy and Science of Materials, University of Oxford, Parks Road, Oxford OX1 3PH, England.

0567-7394/81/040465-07$01.00

potential field of the specimen. Assuming a weak phase object, we find that the second- and higher-order terms in the expansion may be neglected and their analysis follows. Assuming a purely phase object, Cowley (1975) and Fejes (1977) have further shown that the arguments concerning imaging conditions based on the weak-phase-object approximation (WPOA) should also hold for a strong phase object in a qualitative manner, although they fail quantitatively.

The basis of the multi-slice formulation of the dynamical theory of electron diffraction is also based on the assumption of the phase-object approximation (POA) for each hypothetical slice of a crystal and the convolution of such a transmission function with a propagation function as the electron beam propagates from one slice to the next (Cowley & Moodie, 1957). The equivalence of the multi-slice formulation of the dynamical theory and the Bloch-wave formulation has now been firmly established (Goodman & Moodie, 1974; Jap & Glaeser, 1978). It would therefore be interesting to establish the relationship between the intensity distribution in the structure image of a thin crystal and the potential distribution in the crystal, starting from the Bloch-wave formulation of lattice imaging. The result of such an analysis shows that, for a very thin crystal, provided the contrast transfer function is constant for all the beams admitted by the objective aperture, the contrast in the structure image is in a one-to-one correspondence with the projection of the potential distribution (PPD) in the crystal along the beam direction. At a higher approximation, *i.e.* for a relatively thicker crystal, it is shown that the image is proportional to a linear superposition of projected potential distribution, the square of this function and the projected charge density (PCD). Since, for structures whose projections consist of resolvable (*i.e.* non-overlapping) atoms, the variations of all these three functions are in phase, the maxima and minima in the image intensity may be related to the peaks and troughs of the PPD. This correlation is, however, no longer linear and as straightforward as the case where WPOA is applicable.

Some examples of images from a very thin crystal (WPOA), obtained under the condition of constant transfer function for different numbers of beams contributing to the image, are presented. These images show that the true dimensional and angular relationships in the crystal are not reproduced in the image even for a weak phase object at the proper defocus unless a large number of beams effectively contribute to the image. The reason for the deviation in the experimental images is probably that, because of spatial and temporal loss of coherence, not enough diffracted beams contribute to the image for a true representation of the PPD. Simulated images from thicker crystals show that the same deviations are also present in these images.

2. Contrast in lattice images

The intensity, $I(\mathbf{r})$, at a point $\mathbf{r}$ in the image plane is given by (Pirouz, 1979, 1980)

$$I(\mathbf{r}) = \frac{1}{M^2} \sum_j \sum_l B^{jl} \times \sum_g \sum_G D^{jl}_{gG} \exp\left[\frac{2\pi i}{M} (\mathbf{g} - \mathbf{G}).\mathbf{r}\right], \quad (1)$$

where

$$B^{jl} = \psi^{(j)} \psi^{*(l)} \exp(2\pi i t \Delta\gamma^{jl}), \quad (2a)$$

$$D^{jl}_{gG} = C^{(j)}_g C^{*(l)}_G \exp\{-2\pi i[\chi(\mathbf{g} + \mathbf{K}_{\parallel}) - \chi(\mathbf{G} + \mathbf{K}_{\parallel})]\}. \quad (2b)$$

In these equations, M is the magnification, $\psi^{(j)}$ is the excitation amplitude of the jth Bloch wave, $C^{(j)}_g$ is the amplitude of the jth Bloch-wave component of the gth diffracted beam, $\Delta\gamma^{jl}$ is the distance between j and l branches of the dispersion surface, $\mathbf{K}_{\parallel}$ is the tangential component of the incident wave vector (parallel to the zero-order Laue zone) and $\chi(\mathbf{g})$ is the aberration function defined as follows:

$$\chi(\mathbf{g}) = \frac{C_s g^4}{4K_0^3} - \frac{g^2 \Delta f}{2K_0},$$

where $\mathbf{K}_0$ is the incident wave vector, C_s is the coefficient of spherical aberration and Δf is the defocus. The parameter $\gamma^{(j)}$ in (1) is related to the normal component of the Bloch-wave vector, $k_z^{(j)}$, by the following relation:

$$\gamma^{(j)} = k_z^{(j)} - K_z,$$

where K_z is the normal component of the incident wave vector.

The intensity, $I(\mathbf{r})$, may be expressed as the sum of two parts: a constant background intensity, I_B, and a contrast term, $\Delta I(\mathbf{r})$, above or below the background, as follows:

$$I(\mathbf{r}) = I_B + \Delta I(\mathbf{r}),$$

where I_B and $\Delta I(\mathbf{r})$ are given by the $g = G$ and $g \neq G$ terms in (1) respectively.

The above equations show that, in order to calculate the intensity of a lattice image, we need to know the excitation coefficients, $\psi^{(j)}$, the wave amplitudes, $C^{(j)}_g$, and the parameter $\gamma^{(j)}$ of each Bloch wave j. In general, $C^{(j)}_g$ and $\gamma^{(j)}$ are obtained from the following eigenvalue equation (Hirsch, Howie, Nicholson, Pashley & Whelan, 1965):

$$A\mathbf{C}^{(j)} = \gamma^{(j)} \mathbf{C}^{(j)}, \quad (3)$$

where $\mathbf{C}^{(j)}$ is a column vector whose elements are the

wave amplitudes of a particular Bloch wave j. The elements of matrix A are given by (Pirouz, 1974)

$$\alpha_{ii} = \frac{1}{2K_z}(g_i^2 + 2\mathbf{g}.\mathbf{K}_{\|}) \tag{4a}$$

$$\alpha_{ij} = -\frac{1}{2K_z} U_{i-j},\ i \neq j. \tag{4b}$$

U_i is the Fourier coefficient of the ith term in the following series expansion of the crystal potential, $V(\mathbf{r})$:

$$V(\mathbf{r}') = \frac{h^2}{2me} \sum_g U_g \exp(2\pi i\, \mathbf{g}.\mathbf{r}'), \tag{5}$$

where $\mathbf{r}'$ is a position vector in the crystal. As (4) shows, the matrix A is Hermitian, thus implying that the matrix of wave amplitudes, C, is unitary. It can then be easily shown that

$$\psi^{(J)} = C_0^{*(J)}. \tag{6}$$

In structure imaging, nearly always, the incident beam is parallel to a low-index zone of the crystal under observation. Hence, the zero-order Laue zone is parallel to the crystal surface and $\mathbf{K}_{\|} = 0$.

3. Thin-crystal approximations

Let us expand the exponential in (2a) in terms of powers of t:

$$\exp(2\pi i t \Delta\gamma^{jl}) = 1 + 2\pi i t \Delta\gamma^{jl} - 2\pi^2 t^2 (\Delta\gamma^{jl})^2 + \ldots. \tag{7}$$

Each power of t in the above expansion gives rise to a contrast term in (1). Hence we may write

$$\Delta I(\mathbf{r}) = \Delta I_1(\mathbf{r}) + \Delta I_2(\mathbf{r}) + \ldots + \Delta I_n(\mathbf{r}) + \ldots, \tag{8}$$

where ΔI_n refers to the t^n term in (7).

3.1. *The PPD approximation*

In this approximation, we assume a very thin crystal, ($t \ll 1/\Delta\gamma^{jl}$), such that the second and higher powers of t in (7) may be neglected, *i.e.*

$$\exp(2\pi i t \Delta\gamma^{jl}) \simeq 1 + 2\pi i t \Delta\gamma^{jl} \ldots. \tag{9}$$

Substituting (9) in (1) and rearranging, we get:

$$\Delta I_1(\mathbf{r}) = \frac{1}{M^2} \sum_{g \neq G} \sum \exp\left[\frac{2\pi i}{M}(\mathbf{g}-\mathbf{G}).\mathbf{r}\right] \times \exp\{-2\pi i[\chi(\mathbf{g}) - \chi(\mathbf{G})]\} \times \left\{ \sum_j C_0^{*(J)} C_g^{(J)} \sum_l C_o^{(l)} C_G^{*(l)} + 2\pi i t \left[\sum_j C_0^{*(J)} \gamma^{(J)} C_g^{(J)} \sum_l C_0^{(l)} C_G^{*(l)} - \sum_l C_0^{(l)} \gamma^{(l)} C_G^{*(l)} \sum_j C_0^{*(J)} C_g^{(J)} \right] \right\}.$$

Making use of the orthogonality relation

$$\sum_j C_g^{(J)} C_G^{*(J)} = \delta_{gG},$$

where δ_{gG} is the Kronecker delta, we can see that all the terms in the summation over G are zero except for the term $G = 0$. Also, since $g \neq G$, we have $g \neq 0$ and $\sum_j C_0^{*(J)} C_g^{(J)} = 0$. Hence, the above equation for the image contrast reduces to

$$\Delta I_1(\mathbf{r}) = \frac{2\pi i t}{M^2} \left\{ \sum_{g \neq 0} \exp\left(\frac{2\pi i}{M}\mathbf{g}.\mathbf{r}\right) \times \exp[-2\pi i \chi(\mathbf{g})] \sum_j C_0^{*(J)} \gamma^{(J)} C_g^{(J)} - \sum_{g \neq 0} \exp\left(-\frac{2\pi i}{M}\mathbf{g}.\mathbf{r}\right) \times \exp[2\pi i \chi(\mathbf{g})] \sum_j C_0^{(J)} \gamma^{(J)} C_g^{*(J)} \right\}. \tag{10}$$

Now let us represent the gth row of the matrix A by the row vector $\mathbf{A}_g$. In this case (3) and (4) show that

$$\gamma^{(J)} C_g^{(J)} = \mathbf{A}_g \mathbf{C}^{(J)} = \sum_k \alpha_{gk} C_k^{(J)}$$

and

$$\sum_j C_0^{*(J)} \gamma^{(J)} C_g^{(J)} = \sum_k \alpha_{gk} \sum_j C_0^{*(J)} C_k^{(J)} = \alpha_{g1} = -\frac{1}{2K_2} U_g.$$

Similarly,

$$\sum_j C_0^{(J)} \gamma^{(J)} C_g^{*(J)} = \alpha_{g1}^* = \alpha_{1g} = -\frac{1}{2K_z} U_{-g}.$$

Substitution in (10), with the fact that $\chi(g)$ is an even function, then gives

$$\Delta I_1(\mathbf{r}) = -\frac{2\pi t}{M^2 K_z} \sum_{g \neq 0} U_g \exp\left(\frac{2\pi i}{M}\mathbf{g}.\mathbf{r}\right) \sin[2\pi\chi(g)]. \tag{11}$$

Note that $\mathbf{r}$ is a vector perpendicular to the incident beam direction.

Now, the projection of the potential distribution along the beam direction, $V_p(\mathbf{r})$, may be Fourier expanded as follows:

$$V_p(\mathbf{r}) = \frac{h^2}{2me}[U_0 + \sum_{g \neq 0} U_g \exp(2\pi i \mathbf{g}.\mathbf{r})], \tag{12}$$

where U_0 is the mean inner potential. A comparison of (11) and (12) shows that, for a very thin crystal, the

image contrast is in a one-to-one correspondence with the PPD provided that

$$\sin[2\pi\chi(g)] = \text{constant}, \tag{13}$$

for all the reflections admitted by the objective aperture. Positive and negative values of the constant give images with reverse and normal contrast respectively. The image obtained from a very thin crystal with condition (13) satisfied may be called a 'PPD-type image'.

3.2. *The second-order approximation*

Let us now consider $\Delta I_2(\mathbf{r})$ in (8), which corresponds to the contrast term due to the second power of t in (7). With the same type of analysis as in § 3.1, it can be shown that

$$\begin{aligned}\Delta I_2(\mathbf{r}) = -\frac{2\pi^2 t^2}{M^2}\Bigg(&\sum_{g\neq 0}\exp\left(\frac{2\pi i}{M}\mathbf{g}.\mathbf{r}\right)\exp[-2\pi i\chi(g)]\\ &\times\sum_j \gamma^{(j)^2} C_0^{*(j)} C_g^{(j)}\\ &+\sum_{g\neq 0}\exp\left(-\frac{2\pi i}{M}\mathbf{g}.\mathbf{r}\right)\exp[2\pi i\chi(g)]\\ &\times\sum_j \gamma^{(j)^2} C_0^{(j)} C_g^{*(j)}\\ &-\frac{1}{2K_z^2}\sum_{g\neq G}\sum U_g U_G^*\exp\left[\frac{2\pi i}{M}(\mathbf{g}-\mathbf{G}).\mathbf{r}\right]\\ &\times\exp\{-2\pi i[\chi(g)-\chi(G)]\}\Bigg).\end{aligned} \tag{14}$$

With a well known relationship for a diagonalizable matrix such as A:

$$A^k = C^{-1}\gamma^k C,$$

where γ is the diagonal matrix of eigenvalues, we can see that

$$\sum_j C_0^{*(j)}\gamma^{(j)^2} C_g^{(j)} = \alpha'_{g0}$$

and

$$\sum_j C_0^{(j)}\gamma^{(j)^2} C_g^{*(j)} = \alpha'_{0g},$$

where α'_{g0} and α'_{0g} are elements of the A^2 matrix:

$$\alpha'_{g0} = \sum_k \alpha_{gk}\alpha_{k0} = \frac{1}{4K_z^2}(-g^2 U_g + \sum_{k\neq g\neq 0} U_k U_{g-k}),$$

$$\alpha'_{0g} = \sum_k \alpha_{0g}\alpha_{kg} = \frac{1}{4K_z^2}(-g^2 U_g^* + \sum_{k\neq g\neq 0} U_k^* U_{g-k}^*).$$

Now, the operation of squaring any function is equivalent to the operation of self-convoluting its array of Fourier coefficients (Sayre, 1952):

$$^{sq}U_g = \sum_k U_k U_{g-k}, \tag{15}$$

where $^{sq}U_g$ are the Fourier coefficients of $V_p^2(\mathbf{r})$:

$$V_p^2(r) = \frac{h^4}{4m^2 e^2}\sum_g {}^{sq}U_g \exp(2\pi i\mathbf{g}.\mathbf{r}). \tag{16}$$

Hence, (14) reduces to

$$\begin{aligned}\Delta I_2(\mathbf{r}) = \frac{\pi^2 t^2}{M^2 K_z^2}\Bigg(&2U_0\sum_{g\neq 0} U_g\exp\left(\frac{2\pi i}{M}\mathbf{g}.\mathbf{r}\right)\cos[2\pi\chi(g)]\\ &+\sum_{g\neq 0} g^2 U_g\exp\left(\frac{2\pi i}{M}\mathbf{g}.\mathbf{r}\right)\cos[2\pi\chi(g)]\\ &-\sum_{g\neq 0}{}^{sq}U_g\exp\left(\frac{2\pi i}{M}\mathbf{g}.\mathbf{r}\right)\cos[2\pi\chi(g)]\\ &+\sum_{g\neq G}\sum U_g U_G^*\exp\left[\frac{2\pi i}{M}(\mathbf{g}-\mathbf{G}).\mathbf{r}\right]\\ &\times\exp\{-2\pi i[\chi(g)-\chi(G)]\}\Bigg).\end{aligned} \tag{17}$$

The physical meaning of $\Delta I_2(\mathbf{r})$ becomes clearer if we assume an ideal imaging system for which condition (13) holds and examine the four terms in (17). The first term is just the projected potential distribution multiplied by the mean inner potential of the crystal, U_0. The second term is proportional to the PCD, $\rho_p(\mathbf{r})$, since from Poisson's equation

$$\rho_p(\mathbf{r}) \propto \nabla^2 V_p(\mathbf{r}) = \frac{h^2}{2me}\sum_g g^2 U_g \exp(2\pi i\mathbf{g}.\mathbf{r}).$$

Finally, the third and fourth terms are proportional to the square of the PPD from (16) and because

$$V_p^2(\mathbf{r}) = \frac{h^4}{4m^2e^2}\sum_g\sum_G U_g U_G^*\exp[2\pi i(\mathbf{g}-\mathbf{G}).\mathbf{r}].$$

Hence, we see that, provided condition (13) is satisfied, $\Delta I_2(\mathbf{r})$ is proportional to a linear superposition of the PPD, square of the PPD and the PCD:

$$\Delta I_2(\mathbf{r}) = \alpha V_p(\mathbf{r}) + \beta\rho_p(\mathbf{r}) + \gamma V_p^2(\mathbf{r}), \tag{18}$$

where α, β, γ are constants proportional to t^2. Similarly, the total image contrast, $\Delta I(\mathbf{r}) \simeq \Delta I_1(\mathbf{r}) + \Delta I_2(\mathbf{r})$, is proportional to a linear superposition of $V_p(\mathbf{r})$, $\rho_p(\mathbf{r})$ and $V_p^2(\mathbf{r})$.

Note that if the constant in (13) is equal to ± 1, then $\cos[2\pi\chi(g)] = 0$ and the first three terms in (17) cancel out. In this case, $\Delta I(\mathbf{r})$ will be proportional to the PPD (linear in t) and the square of the PPD (quadratic in t).

Now consider a crystal structure oriented in such a way that the projected potential distribution along the beam direction, $V_p(\mathbf{r})$, consists of a number of resolved (*i.e.* non-overlapping) peaks. For such a structure, and only for such a structure, $V_p^2(\mathbf{r})$ also consists of resolved peaks located at the same positions as the peaks of $V_p(\mathbf{r})$. The only difference is that the peaks of $V_p^2(\mathbf{r})$ are sharper as compared to those of $V_p(\mathbf{r})$. Since the variation of $\rho_p(\mathbf{r})$ is also in phase with $V_p(\mathbf{r})$, (17) shows that there will usually be a one-to-one correspondence between the intensity maxima and minima of the image and the projected potential distribution of the crystal. However, unlike the case of the PPD approximation (§ 3.1), the relationship is no longer linear.

One further simplification arises if we consider a structure whose projection along the beam direction is composed of *identical, resolved* atoms. In this case, we may use a method originally due to Sayre (1952), to show that

$$^{sq}U_g = \theta U_g,$$

where θ is a constant defined as

$$\theta = {}^{sq}f/f,$$

where f is the atomic scattering amplitude for electrons (the value of which corresponds to that of the Fourier transform of an atomic peak) and ^{sq}f is the Fourier transform of a 'squared' peak. In this case, and assuming an ideal imaging system for which $\cos[2\pi\chi(g)] = 0$ for all the contributing beams, (17) shows that the image contrast is only proportional to the PPD and hence is directly interpretable.

In practice, of course, where the lens aberrations are always present, the usual phase alterations further distort the image.

4. Results and discussion

According to (11), the pre-requisites for obtaining a PPD-type image are the following conditions:

(i) a very thin crystal ($t \ll 1/\Delta\gamma^{jl}$);

(ii) $\sin[2\pi\chi(g)]$ = constant for all the reflections contributing to the image.

The values of $\Delta\gamma^{jl}$ which should be considered in condition (i) correspond to the Bloch waves which are most strongly excited in the crystal. Usually, in orientations of high symmetry, which is the case for most structure images, only a few waves are strongly excited and the contribution of the rest of the Bloch waves to the image is quite negligible.

Equation (11) shows that the contrast in a PPD-type image of a crystal is determined by the value of the constant in condition (ii). The contrast is obviously greatest for the constant $= \pm 1$ and reduces to zero for constant $= 0$. This latter condition has been called AFF (aberration-free focus) by Hashimoto, Endoh, Tanji, Ono & Watanabe (1977). In keeping with this terminology, we may call the more general condition (ii) CAF (constant-aberration focus).

Some examples of PPD-type images are shown in Fig. 1 for different numbers of beams admitted by the objective aperture. The calculations are based on (1) with $t = 4$ Å and the condition $\sin[2\pi\chi(g)] = 1$ satisfied for all the beams. An accelerating voltage of 100 kV was assumed and 345 beams were taken into account in the calculation of Bloch-wave vectors and amplitudes. However, utilizing the symmetry of the crystal, this number reduces to 94 beams (Pirouz, 1981). Ten levels of greyness, dividing the interval between the maximum and minimum intensities, were used in the simulation of images. The dark regions in all the images correspond to regions of high electron density. Hence, these images correspond to the negative (films) in the microscope.

As in the case of germanium, the present examples show that, in order to be able to resolve the closely spaced (1·36 Å) atoms, it is necessary to allow, at least, thirteen beams to interfere (Spence, O'Keefe & Kolar, 1977). An interesting point which emerges from these figures is an elongation of the distance between the closely spaced spots along the [001] axis. The deviation from the correct dimensions decreases with increasing number of beams contributing to the image. Thus, in going from Fig. 1(*c*) (13 beams) to Figs. 1(*d*) (19 beams), 1(*e*) (23 beams) and 1(*f*) (43 beams), the ratio of the distance between the closely spaced spots to the lattice constant in the [001] direction decreases approximately from 0·3 to 0·27, 0·26 and finally 0·25, which is the structurally correct ratio. This elongation may be also seen in the experimental structure images of silicon (Izui, Furuno & Otsu, 1977) and cadmium telluride (Yamashita, Ponce, Pirouz & Sinclair, 1981). Since the images in Fig. 1 are PPD-type images, this relative elongation is, clearly, not due to electron-optical factors, but, rather, is a consequence of not taking sufficient terms in the Fourier series (12) for a true representation of the potential distribution.

It is well known that factors such as mechanical instabilities and fluctuations in the objective lens current, accelerating voltage and emission source current introduce incoherencies in the electron beam. In the case of weak phase objects, envelope functions have been introduced by Frank (1973) and Fejes (1977) to take the effects of beam convergence and chromatic aberrations into account. However, as O'Keefe (1979) and Ishizuka (1980) have pointed out, such envelope functions should not be applied to strongly scattering objects as it is necessary to include the cross-product terms. In any case, such incoherencies effectively cut off the contribution of higher-order beams [although they may introduce periodicities not due to the structural periodicity but to interference between scattered waves (Ishizuka, 1980)]. It may therefore be possible to use the size of the deviation from true dimensionality in structure images of a known crystal

to get a rough estimate of the influence of beam coherency on the images.

As mentioned previously, the negative and positive values of the constant in (13) give images with normal and reverse contrast respectively. Figs. 2(*a*) and 2(*b*) show these two types of images obtained with the constant -1 and $+1$ respectively.

As Cowley & Iijima (1972) have emphasized, the WPOA, or equivalently the PPD approximation in this paper, is a poor approximation and does not have much practical relevance for most crystal structure imaging. Even so, such an approximation could be useful as a reference point. The second-order approximation, discussed in §3·2, could have some limited application in

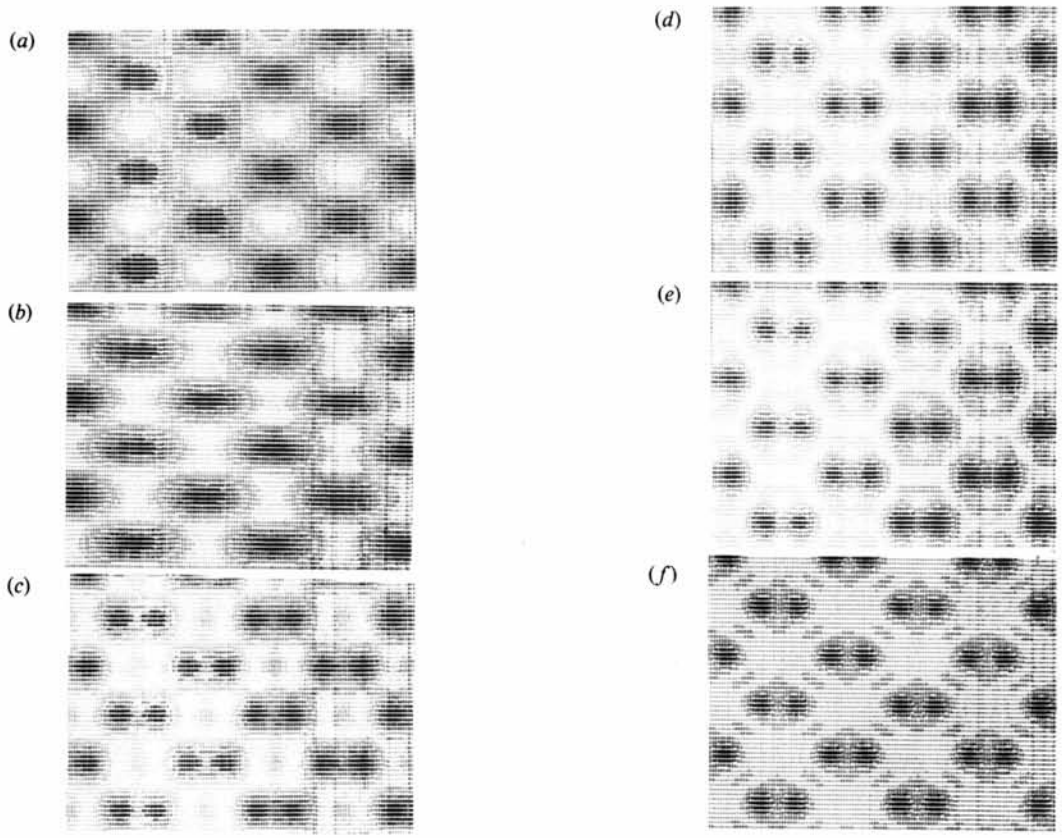

Fig. 1. PPD-type images with different numbers of beams contributing to the image. $t = 4$ Å; $\sin[2\pi\chi(g)] = -1$ for all beams. (*a*) 5 beam; (*b*) 9 beam; (*c*) 13 beam; (*d*) 19 beam; (*e*) 23 beam; (*f*) 43 beam.

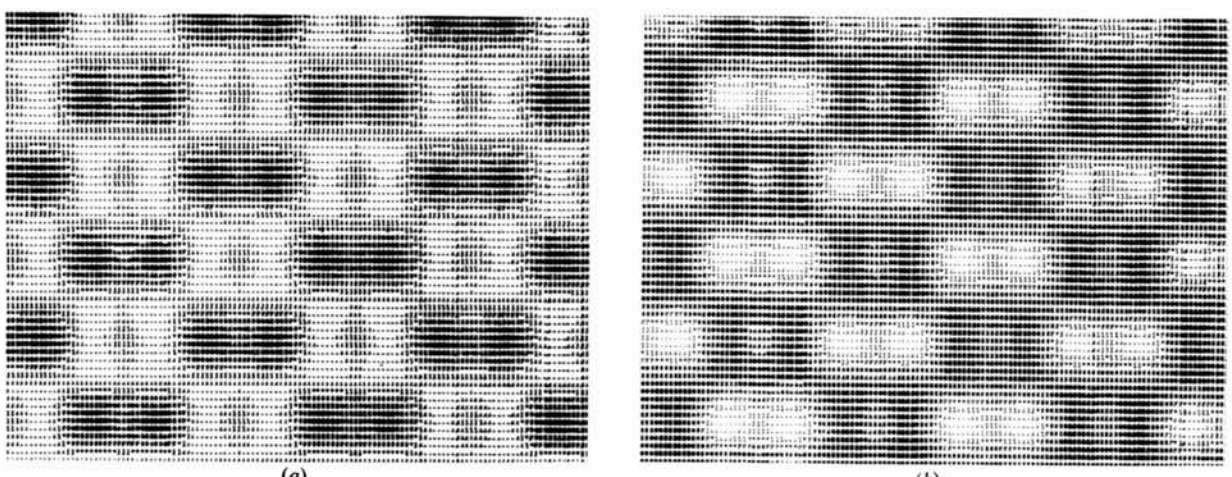

Fig. 2. 13-beam PPD-type images with $t = 4$ Å. (*a*) Normal contrast, $\sin[2\pi\chi(g)] = -1$; (*b*) reverse contrast, $\sin[2\pi\chi(g)] = +1$.

interpreting images, although even this approximation is severely limited both in terms of the crystal thickness and the imaging conditions. Equation (18) was obtained for an ideal imaging system for which condition (13) holds. Even for such an imaging system and assuming that the structure consists of resolved peaks, (18) is interpretable only if the *projected* structure along the beam direction consists of resolved peaks. This may explain the necessity of very accurate alignment of the beam along the zone axes for obtaining interpretable structure images. Even if the structure consists of resolved peaks, a slight tilt may be sufficient to overlap the projected peaks and in that case the location of peaks of $V_p^2(\mathbf{r})$ may not be at the same positions as the peaks of $V_p(\mathbf{r})$. Consequently, the maxima and minima of the image will not have a direct correlation with the variations of the PPD. Conversely, the overlap of the peaks along the directions parallel to the incident beam is not important. It is only the projected potential distribution which should consist of resolved peaks.

We should mention that, within their range of validity, which is determined by the relative values of t and $1/\Delta\gamma^{jl}$ for the most excited Bloch waves, (11) and (17) may be used to calculate the image contrast, $\Delta I(\mathbf{r})$ [$\simeq \Delta I_1(\mathbf{r}) + \Delta I_2(\mathbf{r})$]. The calculations only involve summations over Fourier coefficients of potential and thus obviate the need for computations of Bloch wave vectors and amplitudes.

Finally, in Fig. 3, we have shown computed thirteen-beam images of a silicon crystal at two different thicknesses (t = 60 and t = 285 Å). The accelerating voltage is assumed to be 100 kV with the objective lens having a C_s of 0·7 mm and an underfocus of 670 Å. 345 beams were used in the Bloch-wave calculations as before. These images, no longer of PPD type, still exhibit the same kind of deviations from true angular and dimensional proportions.

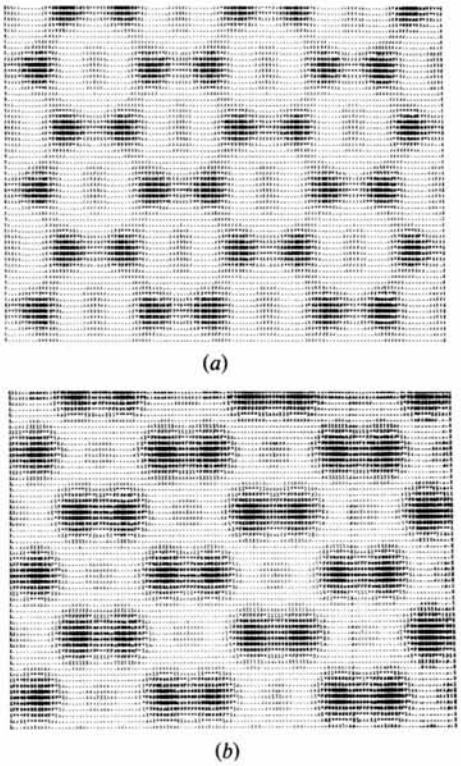

Fig. 3. A typical 13-beam structure image of (*a*) a thin crystal, t = 60 Å, and (*b*) a relatively thick crystal, t = 285 Å, under real operating conditions. 100 kV, C_s = 0·7 mm, Δf = 670 Å.

It is a pleasure to thank Professor J. M. Cowley for his critical reading of the manuscript and his useful suggestions in the preparation of this paper. I am also grateful to Professor Robert Sinclair for supporting this work while the author was visiting Stanford University. Financial support for the setting up of computer programs to do structure image calculations was provided by the Department of Materials Science and Engineering in Stanford University.

References

COWLEY, J. M. (1975). In *Electron Microscopy and Microbeam Analysis*, edited by B. M. SIEGEL & D. R. BEAMAN, pp. 3–15. New York: John Wiley & Sons.

COWLEY, J. M. & IIJIMA, S. (1972). *Z. Naturforsch. Teil A*, **27**, 445–451.

COWLEY, J. M. & MOODIE, A. F. (1957). *Acta Cryst.* **10**, 609–619.

FEJES, P. L. (1977). *Acta Cryst.* A**33**, 109–113.

FRANK, J. (1973). *Optik (Stuttgart)*, **38**, 519–536.

GOODMAN, P. & MOODIE, A. F. (1974). *Acta Cryst.* A**30**, 280–290.

HASHIMOTO, H., ENDOH, H., TANJI, T., ONO, A. & WATANABE, E. (1977). *J. Phys. Soc. Jpn*, **42**, 1073–1074.

HIRSCH, P. B., HOWIE, A., NICHOLSON, R. B., PASHLEY, D. W. & WHELAN, M. J. (1965). *Electron Microscopy of Thin Crystals*. London: Butterworths.

ISHIZUKA, K. (1980). *Ultramicroscopy*, **5**, 55–65.

IZUI, K., FURUNO, S. & OTSU, H. (1977). *J. Electron Microsc.* **26**, 129–132.

JAP, B. K. & GLAESER, R. M. (1978). *Acta Cryst.* A**34**, 94–102.

O'KEEFE, M. A. (1979). *Proceedings, 37th Annual Meeting of the Electron Microscope Society of America*, edited by G. W. BAILEY, pp. 556–557. Baton Rouge, Louisiana: Claitor.

PIROUZ, P. (1974). *Z. Naturforsch. Teil A*, **29**, 1188–1197.

PIROUZ, P. (1979). *Optik (Stuttgart)*, **54**, 69–74.

PIROUZ, P. (1980). *Philos. Mag.* **41**, 33–40.

PIROUZ, P. (1981). Submitted to *Phys. Status Solidi.*

SAYRE, D. (1952). *Acta Cryst.* **5**, 60–65.

SPENCE, J. C. H., O'KEEFE, M. A. & KOLAR, H. (1977). *Optik (Stuttgart)*, **49**, 307–323.

YAMASHITA, T., PONCE, F., PIROUZ, P. & SINCLAIR, R. (1981). In preparation.